

RESEARCH ARTICLE

Gaze Exploration Index (GE i)-Explainable Detection Model for Glaucoma

SAJITHA KRISHNAN¹, J. AMUDHA¹, AND SUSHMA TEJWANI²¹Department of Computer Science and Engineering, Amrita School of Engineering, Amrita Vishwa Vidyapeetham, Bengaluru 560035, India²Narayana Nethralaya, Bommasandra, Bengaluru 560010, India

Corresponding authors: Sajitha Krishnan (k_sajitha@blr.amrita.edu) and J. Amudha (j_amudha@blr.amrita.edu)

This work involved human subjects or animals in its research. Approval of all ethical and experimental procedures and protocols was granted by the Narayana Nethralaya, Narayana Health City, Bengaluru.

ABSTRACT Glaucoma is a type of visual impairment that is caused due to damage in the optic nerve. The vision loss increases from the peripheral vision towards the central vision, leading to blindness if untreated. The proposed approach is a Computer-Aided Detection (CADE) system using deep learning to screen visual field loss in glaucoma patients while performing different day-to-day activities such as searching objects, viewing photographs, etc. Incorporating an eye-tracking device helps to identify eye movements of glaucoma patients while performing different activities. Different day-to-day activities are depicted in the form of visual exploration tasks. CADE system fuses performance parameters and eye gaze parameters during visual exploration tasks onto images, to guide health care professionals of primary eye care centers in glaucoma screening. The pertinent eye gaze and performance parameters are visualized in the form of three fusion maps: Gaze Fusion Map (GFM), Gaze Fusion Reaction Time (GFRT) map, Gaze Convex Hull Map (GCHM), which are the outcomes of different visual exploration tasks. In addition, the explainability techniques applied in CADE generated Gaze Exploration - index (GE-i) that discriminates glaucoma and normal.

INDEX TERMS Glaucoma, eye gaze, visual attention, explainable computer aided detection, visual field loss.

I. INTRODUCTION

Visual impairment or vision loss is the decreased ability to see, which is not correctable using glasses or lenses and leads to difficulties with day-to-day activities [1]. The causes of visual impairment are refractive errors, cataract, glaucoma, age-related macular degeneration, etc. Glaucoma is the second leading cause of blindness after cataract. One-fifth of the glaucoma burden is in India, and the sad part is that more than 90 percent of glaucoma cases remain undiagnosed, in contrast to 40-60 % in developed countries [2]. Different structural and functional tests are used to assess optic nerve head, thickness of cornea, eye pressure and field of vision. Visual field perimetry is a machine that detects the loss in the central and peripheral field of vision.

In a real-world scene, the peripheral vision prompts saccade (eye movement) or head movement and guides the fovea

to the center for more information. The peripheral vision helps to select information or features, and subsequently, the central vision orients to the region of interest. Visual impairment alters visual attention, because it is the effect of the association of central and peripheral visual function in the interaction of real-world scenes [8], [9].

Visual attention of drivers is measured using Useful Field of View (UFoV). This measure checks whether a participant can focus on the central target, divide attention between objects in the central field of view and peripheral field of view, select a target among distractors in the peripheral field of view, and make a mobility control while driving [3]. Mild glaucoma patients with less visual field loss (loss of part of the visual field) get good UFoV scores [4]. They compensate for the defect in the position of the visual field by performing more exploration in the eye gaze patterns, such as more fixation and higher saccade/sec while driving [5]–[7]. It should also be noted that all glaucoma patients may not show exploratory search

The associate editor coordinating the review of this manuscript and approving it for publication was Mingbo Zhao¹.

to compensate visual field loss while performing different activities.

The patients who notice difficulty in their day-to-day tasks undergo diagnosis, treatment, and social rehabilitative programs to overcome their challenges [1]. However, eye care services are not well utilized due to accessibility, affordability, and availability of services [9], [10]. Different tests are available in tertiary hospitals to diagnose glaucoma, but there is an under utilization of such services in rural areas. A feasible solution is needed to perform glaucoma tests in the primary eye centers.

Researchers investigate the influence of eye movement patterns of glaucoma people during the performance of day-to-day activities. This knowledge helps to create a screening test that checks people's visual attention in primary eye care centers and then refers to diagnosing the disease in the higher tier of hospitals. The screening test is incorporated with a computer-aided detection model that discriminates between glaucoma and normal. The explainability techniques applied in the CADe model helped to understand the relevant features that contributed to the prediction of glaucoma.

The outline of the paper is as follows. Section 2 includes eye gaze measures and their use in the diagnosis of glaucoma. Section 3 explains methodology of the proposed system. Section 4 shows results and section 5 explains the discussion of various results. The paper concludes in Section 6.

II. LITERATURE SURVEY

Plenty of studies have reported that severe glaucoma patients show a decline in visual function ability tasks such as reading newspapers, climbing stairs, searching objects, interacting with people, performing leisure activities, dark adaptation, and other outdoor tasks, etc. [11]. They face loss of employment, less productivity, and treatment costs [1]. Researchers worldwide have found variations in eye movement patterns of glaucoma participants while performing visual exploration tasks such as reading, visual search, face recognition, watching TV and video, viewing images, driving, walking, and shopping to understand visual functional deficits of glaucoma patients and how it impacts the quality of life [45], [46]. The research works investigated different tasks in their experiment using low-end, medium-end, and high-end eye trackers.

A visual search experiment reported that the number of saccades per trial, saccade amplitude, saccade size, and fixation duration do not correlate with peripheral visual field loss [15]. Glaucoma patients compensated visual field loss by changing the direction of saccades during visual search. Research works also investigated the visual search behavior of individuals in driving scenes. Glaucoma patients show a low number of fixation and smaller saccades, which show that visual search behavior is diminished in them [16]. Studies show that only a few old glaucoma patients and young glaucoma patients do compensatory patterns by making more saccades or head movements.

The signature of vision loss is generated using saccades landing in the region of the visual field, and it can

discriminate between glaucomatous and normal visual field. However, the characteristics of the saccadic map with the field loss are not linked [17]. Since there are confounding factors such as personality and engagement towards screen-based tasks, experiments are also conducted to compare eye movement patterns between each participant's worse and less glaucoma-affected eye. Less glaucoma-affected eye made many revisits towards the region of interest and created less fixation distribution than worse glaucoma-affected eye [18]. There is a limitation in CADe system which incorporates low-cost eye tracker. Restriction in the visual field is implied in glaucoma patients during free-viewing images and videos, which can be identified as signatures to discriminate between glaucoma and normal [17]. More research works are needed to find the correlation between clinical measures and eye gaze parameters to screen the disease in the early stages.

Clinical tests are always performed in laboratory-based conditions, where glaucoma patients do not show much difference from normal people. But glaucoma patients report difficulty in performing day-to-day activities even with mild impairment [12]. Several eye movement studies investigated to understand the functional deficits of the clinical population. In dynamic scenes such as driving, more saccadic eye movements and head movements are used to overcome the challenges of visual field defect [19], [20], [21]. Despite the compensatory behavior, they showed a slower response to hazards [22], [23], [24]. Eye movement scanning of young participants is different from the older adults with glaucoma in the driving scenes [26].

In screen-based static scenes such as watching TV and visual search, the compensatory behavior of glaucoma patients is different or absent concerning the challenge of the restricted field of vision [19]. In some studies, compensatory behavior such as more significant number of saccades per sec and saccade amplitude to show good performance while shopping [26]. The group showed the same eye movement behavior for good performance in image viewing [27]. Conversely, in another computer-based task, the group ignores the region where visual field loss is present and they do not focus on all parts of the scene [15], [19], [26], [28], [30].

Glaucoma patients show altered eye movement behavior compared to the normal population while watching TV [17]. Apart from clinical testing, knowledge about quality-of-life (QoL) of glaucoma patients helps to understand the progression of the disease [31]. Thus awareness of the disease improves the QoL utilizing compensatory head and eye movements towards the visual field loss. Different studies have shown a correlation between clinical measures and eye gaze parameters in glaucoma patients than normal participants. However, more research is required to understand the influence of severity in the visual field loss in eye movement behavior. Different studies have shown a correlation between clinical measures and eye gaze parameters in glaucoma patients than normal participants. However, more research is required to understand the influence of severity in the visual field loss in eye movement behavior.

The advancement of artificial intelligence in eye care delivery is quite promising [42]–[44]. But the barrier of the black-box approach of many machine learning models are excised by the introduction of Explainable Computer Aided Diagnosis (CADx) and Detection System (CADE). Several research works have designed trustworthy detection system based on the amalgamation of clinical measures using functional and structural modalities and deep learning model [33], [47], [48]. Cup-disk-ratio (CDR) and morphological features from fundus images are fed to the convolution neural network to create CADE and CADx systems, which can assist clinicians [32], [34]. The explainability techniques are utilized to analyze the performance of the different machine learning models. The same concept is also applied to understand the influence of different clinical parameters in creating glaucoma diagnosis and detection systems [33]. The interpretability of feature extraction and explainability of different machine learning models make CADE and CADx more sophisticated and reliable.

The proposed system urged the interpretability of different eye gaze features to understand how different subgroups of glaucoma utilized them in the performance of day-to-day activities. The present work also investigated the influence of age and severity on performance during different tasks. This was demonstrated by comparing the performance of glaucoma participants during the visual exploration tasks and understand whether compensatory eye movement patterns reflect in such different tasks. The proposed Computer Aided Detection (CADE) helps to screen glaucoma patients in primary eye care centers.

III. METHODOLOGY

A. RATIONALE OF THE STUDY

The proposed system is an explainable Computer-Aided Detection (CADE) system that highlights what-if questions of glaucoma screening. The present work addresses the following questions.

- Are exploratory gaze patterns of the same participant reflect in all tasks?
- What are the relevant eye gaze measures and performance measures that contribute the prediction of glaucoma?
- Can we formulate a screening index that discriminates glaucoma and normal?

B. STUDY DESIGN

The overview of the architecture of Gaze Exploration-index (GE-i) Explainable Detection Model is shown in the figure 1. The proposed system is designed with data acquisition, feature analysis and clinical validation, model creation, explainability, visualization and finally outputs the screening index. The system comprised of 4 main modules:

- 1) Visual Exploration Tasks - The module is based on three day-to-day tasks: simple dot (T1) task, visual search (T2) task and free-viewing (T3) task. The system first presented a task which analyzed the performance

of each eye, and identified the more defected eye and less defected eye. This subsequently checked the contribution of binocular vision in the performance during day-to-day tasks such as visual search and image viewing and how they compensate for their visual field loss.

- 2) Estimation of eXtensive Gaze and Performance (EXGP) module - The module constituted open-source software and customized software. The open-source software evaluated basic eye gaze measures and customized evaluated derived parameters. Based on these eye gaze measures, EXGP module estimated task performance measures. Thus the module estimated 28 parameters, which included eye gaze parameters and performance parameters of different participants after viewing visual exploration tasks. The output of the module is the EXGP feature set.
- 3) EXGP Feature Analysis - The EXGP feature set was analyzed based on severity grade and age. The analysis of feature set was validated based on certain clinical measures. The feature analysis was based on statistical measures.
- 4) Explainable – Detection Model - EXGP feature set is fed to Deep Neural Network (DNN), which is included in the Explainable – Detection Model or Computer-Aided Detection model (CADE). DNN predicted any unseen data as glaucoma or not. The accuracy of the model is based on the feature relevance. The explainability of the model was performed in a dashboard in the form of various plots such as waterfall plots, contribution plots etc. The dashboard is also designed to generate screening index called Gaze Exploration-index (GE-i). The module comprised Gaze Exploration Visualization, that is meant for different visual exploration tasks (T1, T2 and T3) in the form of fusion maps.

Participants were engaged and oriented to different tasks displayed on the laptop screen. The underlying computer-aided detection model has generated screening index and created fusion maps, which utilized the information based on task performance and eye movement behavior. The study estimated exploratory gaze patterns that reflect in all tasks for the glaucoma group.

C. PARTICIPANTS

The prospective hospital-based cross-sectional study which is conducted in Narayana Nethralaya, Narayana Health City, Bengaluru is ethically approved by Ethics Committee of the hospital. The purpose of the experiment was explained and different participants signed the consent sheet, and followed by which he/she was invited for the study. The study is carried on participants diagnosed with glaucoma by the standard test (clinical evaluation, visual field test, imaging techniques) and the same number of age-related controls, with an age group of 30-70 years and no constraint on gender. The participants were selected during their regular glaucoma screening. After visual field test, the Humphrey Field Analyzer (HFA) with

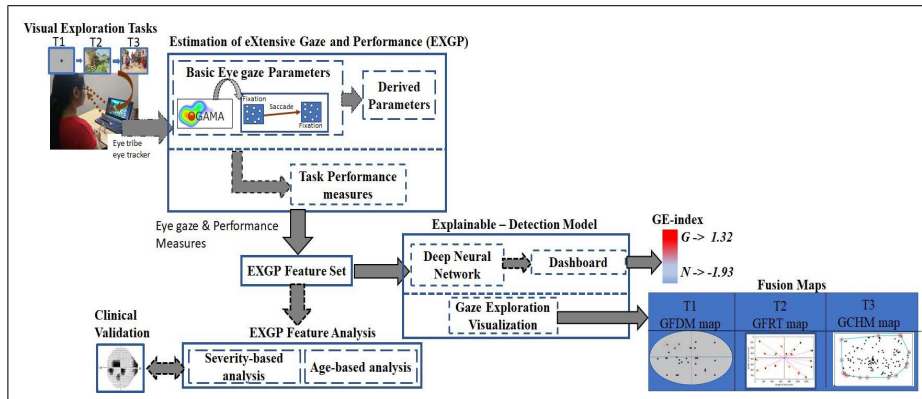


FIGURE 1. Overview of Gaze Exploration - index (GE-i) based explainable detection model.

24-2 program produced a visual field report of different participants. The experimenter maintained a copy of visual field report for clinical validation. A total of 117 participants were recruited. The gaze data of participants are allocated with unique ID: Sub_1, Sub_2,...,Sub_117. Among them, 50 were glaucoma participants, 48 were normal participants, 7 patients had field loss due to other diseases, 2 participants could not complete the experiment due to droopy eyes, and 10 data loss. Thus ninety-eight participants were involved in the experiment.

The study did not include participants who had undergone ocular surgery in the past three months, history with a squint and retinal surgery, and glaucoma suspects. Participants satisfying the inclusion criteria for the study were recruited from outpatient department (OPD) in the hospital. Glaucoma Hemifield Test (GHT) on the perimetry provides the label of ‘outside normal limits’ for glaucoma participants. Glaucoma is diagnosed as mild, moderate, and severe based on the Visual Field Index (VFI) [49]. The flowchart of data collection is shown in the Figure 2.

In the present study, glaucoma were categorized based on Visual Field Index (VFI) [49]. VFI value less than 40 was considered as severe category, VFI between 40 and 60 was considered as moderate category, and VFI value between 60 and 100 was considered as mild category. The subgroups of glaucoma and normal were also identified based on age groups such as young (age less than 45), middle-age (age between 46 and 60) and elder (age greater than 60) subgroups. The subgroup analysis based on severity grade and age-group enlightened the understanding of exploratory gaze patterns in different tasks. The flow diagram of subgroup analysis is shown in the figure 3.

D. EQUIPMENT SETUP

The experimenter or person who had conducted an eye-tracking experiment explained the different tasks in English or in their regional language to the participants. The distance of the participant from the monitor was maintained at 60 cm. A non-invasive eye tracker Eye Tribe 60 Hz

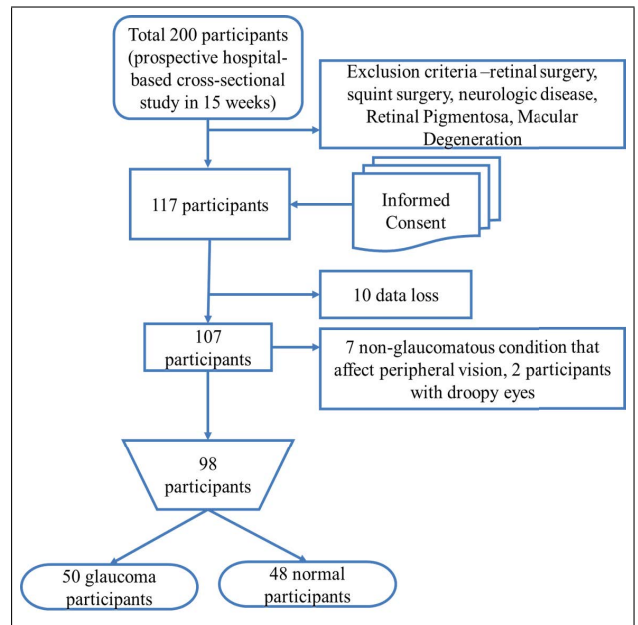


FIGURE 2. Flowchart of data collection.

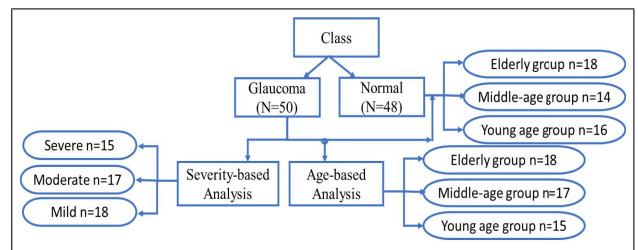


FIGURE 3. Flow diagram of subgroup analysis.

with accuracy 0.5° and spatial resolution 0.1° is attached to the screen. The eye tracker uses infrared illumination to capture the eye movements of the participants when viewing the stimulus on the computer screen. Before starting the experiment, 9-point calibration is run to get the Pupil-Corneal Reflex (PCR) of participants and if required, re-calibration is

done to get the pupil position correctly. The proposed system focused on the strategy of exploratory eye gaze patterns of different participants in different visual exploration tasks.

E. DESCRIPTION OF VISUAL EXPLORATION TASKS

Visual exploration tasks are screen-based tasks that depict specific tasks such as searching for an object, watching T.V., and viewing photographs in daily life. The tasks were based on images that included certain scenes or contained a target with distractors. Participants engaged and explored images based on the instructions given by the experimenter. The images were designed in such a way that the participants should utilize all parts of the screen. Figure 4 shows the sample images of different tasks.

1) SIMPLE DOT TASK

This was the first task (T1), in which the stimulus included a white dot of size 12 pixels. The dots were displayed randomly on the screen. The position of each dot is arranged in four quadrants: Top Left (TL), Bottom Left (BL), Top Right (TR) and Bottom Right (BR). There were 30 images in the task and each image was displayed for 1.5 sec. The participant viewed the image monocularly (each eye separately) and no response was required from them. Figure 4(a) shows a sample image of T1 task.

2) VISUAL SEARCH

The second task (visual search) was a task-oriented activity that included a set of cartoon images, in which each image was displayed on the screen for 20 sec. The image was selected from Bing search engine and a target in the form of 'star' was placed at different positions. The target question was "Find the star in the image"? Participants searched for a target and responded by clicking the mouse button on the target or telling the experimenter the target's position. There were 20 images in the task, which included colour and gray scale images. The target included different modalities such as size (varies between 10 and 14 pixels to match the background), orientation, position, and opacity in four quadrants (TL, TR, BR, BL). There were at least four images in each quadrant. A central dot was displayed for 1 sec after every image. Figure 4(b) shows a sample image of T2 task.

3) FREE-VIEWING TASK

This was the final task (T3), in which no response was required from the participants. The task included 20 images and they observed different salient features such as traffic lights, people, animals, etc. The images were selected from Bing image search engine and CAT2000 benchmark dataset (selected Indian based images). The task included color and gray-scale images and the trial time was 4 sec. The image size was 1366×768 , which was displayed on the full screen. A central dot was displayed for 1 sec after every image. Some images were inverted or applied noise on images to grab the attention of participants to the task. Figure 4(c) shows a sample image of T3 task with social scenes and applied some

noise on it. Figure 4(d) shows a sample image of T3 task with background scenes.

F. ESTIMATION OF EXTENSIVE GAZE AND PERFORMANCE (EXGP) MODULE

The proposed system included a submodule called Estimation of eXtensive Gaze and Performance (EXGP) module. The submodule comprised open-source software OGAMA 5.0 [50] and customized software [35]. OGAMA 5.0 estimated basic eye gaze parameters from the gaze samples from the eye tracker. The basic eye gaze parameters fed to the customized software. The customized software estimated extensive eye gaze parameters or derived parameters to differentiate eye movement behavior between glaucoma and normal. The inclusion of OGAMA open source software in EXGP module is required to calculate basic eye gaze parameters from gaze samples that cannot be calculated using customized software.

1) BASIC EYE GAZE PARAMETERS

The open-source software OGAMA 5.0 preprocessed samples from the eye tracker to remove artefacts and outliers. The software estimated events such as fixations and saccades from the gaze samples from the eye tracker. Fixations were estimated as clusters of still eye movements over a time period. Saccades were estimated as rapid eye movements between fixations.

2) DERIVED PARAMETERS

Since visual exploration tasks such as free-viewing and goal-oriented tasks (visual search) expected different manner of eye movements, the customized software is needed to calculate different comprehensive eye gaze measures from the basic eye gaze parameters. The summary of the relationship of eye gaze parameters with the visual field is depicted in the table 1.

The derived parameters are described as follows:

- Fixation Count (FC) – FC is calculated as the count of fixations done by the participant while viewing a stimulus. Average value of all trials are estimated for each participant. Average FC for visual search and free-viewing tasks are denoted as Star_Avg_FC and fv_Avg_FC respectively.
- Saccade Count (SC) – SC is calculated as the number of saccades made by participant while viewing a stimulus. There can be saccades along a reverse direction called regression. Average of SC for visual search task and free-viewing task are abbreviated as Star_Avg Saccade Count and fv_Avg Saccade Count respectively.
- Saccade rate – It is calculated as the number of saccades made by the participant per second, and it is also known as eye movement rate. Average of SC for visual search task and free-viewing task are denoted as star_Avg Saccade Rate and fv_Avg Saccade Rate respectively.
- Fixation Duration (FD) – The duration taken by the eye to be still at a particular area. While viewing the

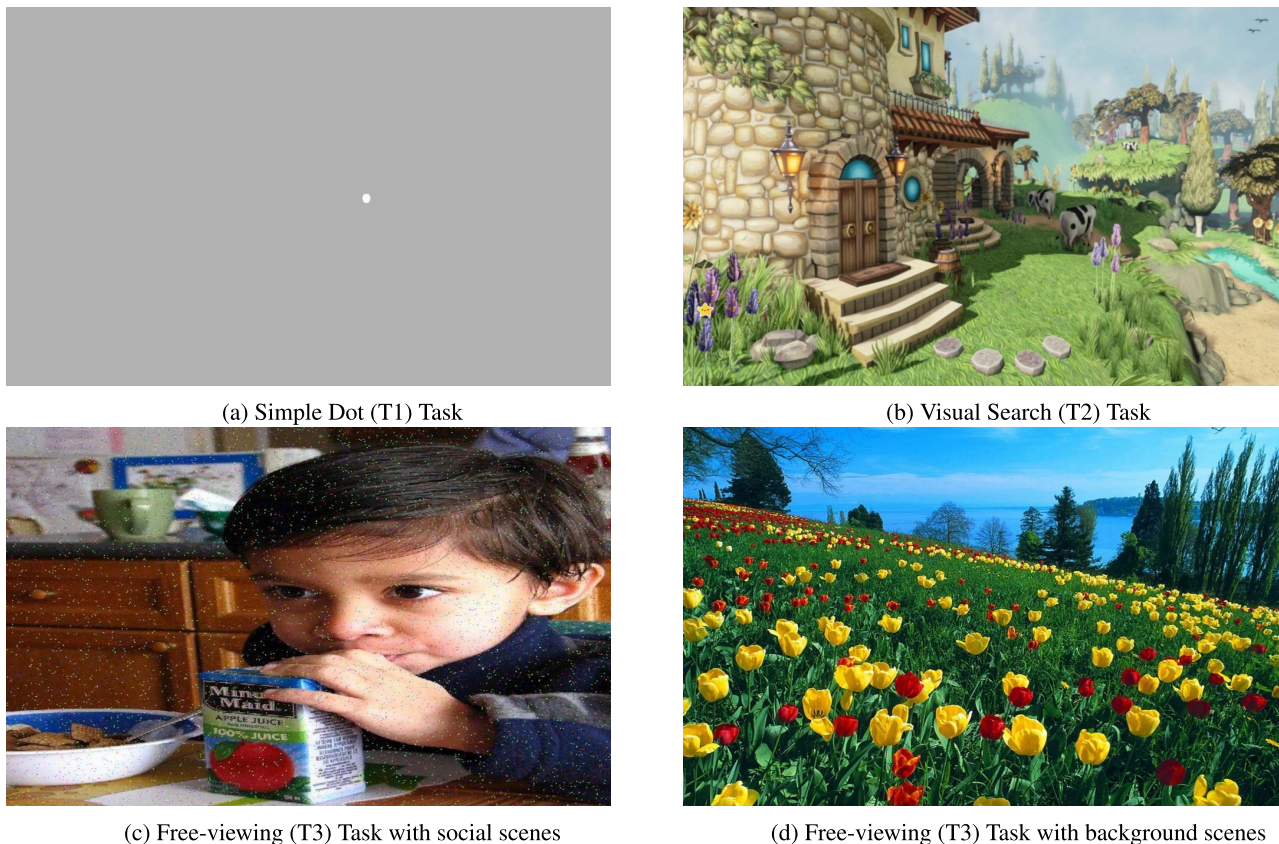


FIGURE 4. Sample of visual exploration tasks.

TABLE 1. Relation of eye gaze measures and its outcome.

Derived Parameters	Definition	Inference
Horizontal and Vertical Ratio (HV-ratio)	Check of dominance of horizontal and vertical saccades	Restriction in the visual field
Scan path Length	Adding Saccade amplitudes in a scan path	
Convex Hull Area	Polygonal space that covers all fixations of a participant	
Saccadic Direction	Direction of saccades	Exploratory eye movement
Fixation Count	Number of fixations	
Saccade Count	Number of saccades towards the region of interest	
Saccade Rate	Number of saccades per second	
Saccade Velocity	Eye movement rate	Visual processing of the stimulus
Fixation Duration	Duration taken by the eye to be still at a particular area	
Fixation/Saccade ratio	Ratio based on saccade amplitude	

stimulus, participants show a smaller number of fixations and higher number of saccade amplitude to understand visual information and later fixation duration will be increased and saccade amplitude will get reduced to understand the semantics of the stimulus. Generally visual field is longer horizontally than vertically. Average of SC for visual search task and free-viewing task are denoted as Star_Avg FD and fv_FD mean respectively.

- Fixation/Saccade ratio (F/S ratio) – It indicates the number of saccades greater than the amplitude threshold divided by the number of saccades smaller than the amplitude threshold. It shows the difference between global scanning and detailed inspection. F/S ratio of

free-viewing and visual search are prefixed with star and fv as star_F/S ratio and fv_F/s ratio respectively.

- Saccade Velocity – Saccade velocity (SV) is the eye movement speed. It is calculated by dividing saccade amplitude by saccade duration. SV of free-viewing and visual search are prefixed with star and fv as star_SV and fv_SV respectively.
- Scanpath Length (SL) - This parameter is calculated by adding saccade amplitudes in a scan path. SL of free-viewing and visual search are prefixed with star and fv as star_SL and fv_SL respectively. The length between fixations are denoted as Fix Conn Length; prefixed with star and fv.

- Saccadic Direction – Saccadic orientation is the direction of saccades and generally while viewing scenes participants show horizontal orientation and the dominance of horizontal and vertical saccades can be inspected using Horizontal and Vertical Ratio (HV-ratio). Saccadic Direction of free-viewing and visual search are prefixed with Star and fv as star_Saccadic direction and fv_Saccadic direction respectively.
- Scanpath - Scanpath is a graph containing fixations as vertices and saccades as edges between vertices.
- Convex Hull Area – It refers to the polygonal space that covers all fixations of a participant across all trials. It shows the shape of the scanpath done by a participant across all trials. Average of convex hull area for visual search task and free-viewing task are denoted as star_Convex Hull Area and fv_Convex Hull Area respectively.

3) PERFORMANCE MEASURES

The performance of participants during visual exploration tasks was estimated based on the parameters from the EXGP module. The monocular performance in simple dot task and binocular performance in visual search task was estimated based on the fixation over the target within the trial time.

The monocular performance of participants in the simple dot task was estimated using average miss. The parameter was calculated by summing up of miss in different trials divided by number of images. It was estimated for each eye such as left eye miss and right eye miss. If the participant could fixate the target, it was considered as seen/hit. The performance measure in simple-dot task is denoted as Dot_Avg Miss.

The task was followed by binocular performance in daily routines tasks such as visual search and free-viewing tasks. The reaction time to identify the target was calculated by clicking the mouse on the region of interest 'star'. The participants could also communicate the experimenter the star's location and fixate on the target for five seconds. The threshold of fixation duration was decided based on the pilot study. The average reaction time was calculated as the summing up of reaction time divided by the number of images. The performance measure in visual search task is denoted as Star_Avg RT.

The free-viewing task was not goal-oriented activity and hence no performance measure was estimated. The extensive eye gaze and performance measures are called feature set of EXGP module. EXGP module outputs *EXGP Feature Set*. The feature set includes 28 features which are fed to analysis framework and detection model.

Mean, standard deviation (in parenthesis) and p-value between glaucoma and normal of different features in EXGP feature set are shown in the Table 2. The p-value <0.05 is shown in boldface manner, that are significant.

The performance measures such as Dot Avg Miss and Star Avg RT is significantly different between glaucoma and normal with $p < 0.001$ and $p < 0.05$ respectively. There is also a significant difference in fixation duration, fixation

count per sec, saccade velocity and fixation connection length with $p < 0.05$ between glaucoma and normal in visual search task. Glaucoma group had taken longer fixation duration than normal with less number of fixation count and that made their performance in visual search poor.

There is also a significant difference in fixation count per second, fixation connection length, convex hull area and saccade rate between glaucoma and normal in free-viewing task. Glaucoma participants showed lower fixation count and less convex hull area than normal participants in free-viewing task.

G. EXGP FEATURE ANALYSIS

EXGP module in the GE-i proposed model estimated 28 parameters, which included 26 comprehensive eye gaze measures estimated during visual search task and free-viewing task altogether, average miss estimated during simple dot task and average reaction time estimated during visual search task. These comprised to form EXGP feature set. The feature set is analysed based on different severity grade subgroups and age-based subgroups. The summary of significance testing is tabulated in Table 3, Table 4 and Table 5, and explained in the subsequent two sections: Severity-based Analysis and Age based Analysis.

1) SEVERITY-BASED ANALYSIS

The glaucoma group was categorized into severe, moderate and mild subgroups for the study purpose. Comparison of eye tracking measures between severe and mild subgroups showed that there is a significant difference in saccade count and saccade rate $p < 0.001$ during both visual search and free-viewing tasks and in the reaction time during visual search. No significant difference has been identified in average miss as well as other eye tracking measures between severe and mild subgroups.

The comparison between moderate and mild subgroups showed that there is a significant difference between saccade count and saccade rate in free-viewing task and visual search task with $p < 0.001$. But no significant difference has identified in other EXGP features. Saccade rate and saccade count were the exploratory eye gaze patterns shown by mild glaucoma subgroups than moderate and severe glaucoma subgroups.

2) AGE-BASED ANALYSIS

Based on age group, the glaucoma group was categorized into elder, middle-age and young subgroups. The comparison between elder and middle age subgroups showed that there is a significant difference in average miss in simple dot task with $p \leq 0.001$ and convex hull area in free-viewing task with p-value 0.037.

Elder and young subgroups showed a significant difference in the performance of average miss and average reaction time with p-value=0.018 and p-value=0.014 respectively. There is a significant difference in fixation duration in both visual search and free-viewing tasks with p-value=0.031 and

TABLE 2. Mean and standard deviation (in parenthesis) of EXGP features and p-value between glaucoma group and normal group.

Sl.No.	EXGP features	Glaucoma	Normal	p-value
1	Dot_Avg Miss	0.6(0.3)	0.2(0.2)	p<0.001
2	Star_Avg RT	7.0(3.6)	5.6(2.9)	0.048
3	Star_Avg FC	5.5(4.7)	6.1(5.4)	0.59
4	Star_Avg FD	309.1(175.2)	240.9(97.7)	0.029
5	star_FC/s	0.6(0.4)	0.9(0.8)	0.0052
6	star_F/S ratio	185.1(141.3)	251.2(209.4)	0.09
7	star_Avg SL	255.9(77.8)	263.1(67.4)	0.64
8	star_Avg SV	1.2(0.9)	1.8(1.1)	0.004
9	star_Fix Conn Length	1391.0(1015.2)	2124.5(1418.5)	0.007
10	star_HV ratio	36.4(131.5)	-6.6(52.9)	0.051
11	star_Saccadic direction	0.1(0.4)	0.4(1.4)	0.20
12	star_Convex Hull Area	3120.2(625.8)	3379.8(584.6)	0.05
13	star_Avg Saccade Count	6.5(4.4)	5.1(3.7)	0.11
14	star_Avg Saccade Rate	1.4(0.3)	1.3(0.3)	0.42
15	fv_FC	4.6(3.2)	6.1(4.3)	0.08
16	fv_FC/s	1.4(0.7)	1.8(0.9)	0.007
17	fv_FD mean	197.1(73.2)	185.3(77)	0.46
18	fv_SD mean	143.4(42.6)	135.5(32.7)	0.33
19	fv_F/s ratio	263.8(169.5)	282.6(208.2)	0.64
20	fv_Avg SL	184.8(95.9)	203.1(84.8)	0.35
21	fv_Avg SV	1.5(1.2)	1.7(1)	0.47
22	fv_Fix Conn Length	734.4(521.3)	1230.3(932.6)	0.003
23	fv_Regressions	0.7(0.3)	0.8(0.5)	0.30
24	fv_HV ratio	571.6(2763.9)	0.4(28.6)	0.18
25	fv_Saccadic direction	0.1(0.5)	0.1(0.2)	0.66
26	fv_Convex Hull Area	2400.7(632.6)	2934.2(463.8)	p<0.001
27	fv_Avg Saccade Count	4.5(3.0)	5.8(3.6)	0.06
28	fv_Avg Saccade Rate	1.6	1.8(0.5)	0.03

TABLE 3. Summary of significance testing and impact in severe glaucoma subgroup.

Visual Exploration Tasks	EXGP Features	Significant Difference	Mild (n=18)	Severe (n=15)	p-value	Impact in Severe Glaucoma Subgroup
Single-Dot (T1) Task	-	-	-	-	-	-
Visual Search (T2) Task	Star_Avg RT	✓	6.5(3.4)	11(3.0)	0.04	Longer reaction time
	star_Avg Saccade Count	✓	5.85(3.79)	3.36(1.45)	p<0.001	Less saccade count during search
	star_Avg Saccade Rate	✓	1.82(0.58)	1.39(1.45)	p<0.001	Less saccade count during search
Free-viewing (T3) Task	fv_Avg Saccade Count	✓	7.35(3.69)	4.30(1.58)	p<0.001	Less saccade count during image-viewing
	fv_Avg Saccade Rate	✓	1.47(0.31)	1.14(0.14)	p<0.001	Less saccade count during image-viewing

p-value=0.035 respectively. Convex hull area in visual search task showed p-value with 0.04 between elder and young subgroups.

No significant difference showed in EXGP features between young and middle-age subgroups. There is significant difference in the performance during tasks between elder and young subgroups. Elderly glaucoma subgroup showed longer fixation duration that led to limited exploration during the performance of both tasks.

H. CLINICAL VALIDATION

Humphrey Field Analyzer (HFA) visual field test is done for left and right eyes separately. The parameters in the visual

field report estimate the retinal sensitivity of each eye, which helps the clinicians to understand functional deficits in terms of the visual field.

- Mean Deviation (MD) - the average deviation from the age-matched normal in terms of retinal sensitivity. The negative values show the presence of the worse field defect.
- Pattern Standard Deviation (PSD) - Clinicians used PSD to understand the irregular depression in the visual field defect. The higher positive values indicate the higher functional loss.
- Visual Field Index (VFI) - the percentage of visual field status. The lower value indicates worse field defects. Glaucoma is diagnosed as mild, moderate, and severe

TABLE 4. Summary of significance testing and impact in moderate glaucoma subgroup.

Visual Exploration Tasks	EXGP Features	Significant Difference	Mild (n=18)	Moderate (n=17)	p-value	Impact in Moderate Glaucoma Subgroup
Single-Dot (T1) Task	-	-	-	-	-	-
Visual Search (T2) Task	star_Avg Saccade Count	✓	5.85(3.79)	3.36(1.45)	p<0.001	Less saccade count during search
	star_Avg Saccade Rate	✓	1.82(0.58)	1.39(1.45)	p<0.001	Less saccade count during search
Free-viewing (T3) Task	fv_Avg Saccade Count	✓	7.35(3.69)	7.0(1.08)	p<0.001	Less saccade count during image-viewing
	fv_Avg Saccade Rate	✓	1.47(0.31)	1.35(0.20)	p<0.001	Less saccade count during image-viewing

TABLE 5. Summary of significance testing and impact in elderly glaucoma subgroup.

Visual Exploration Tasks	EXGP Features	Significant Difference	Young Glaucoma (n=15)	Elder Glaucoma (n=18)	p-value	Impact in Elderly Glaucoma Subgroup
Single-Dot (T1) Task	Dot_Avg Miss	✓	0.403(0.21)	0.70(0.36)	0.018	Increase in miss
Visual Search (T2) Task	Star_Avg RT	✓	4.99(2.4)	8.10(2.8)	0.014	Longer reaction time
	Star_Avg FD	✓	244.7(76.5)	370(109.8)	0.031	Longer fixation duration
	star_Convex Hull Area	✓	3397(300.4)	3000(539.5)	0.04	Smaller area to cover all fixation
Free-viewing (T3) Task	fv_FD mean	✓	171.3(56.8)	204.8(51.0)	0.035	Longer fixation duration

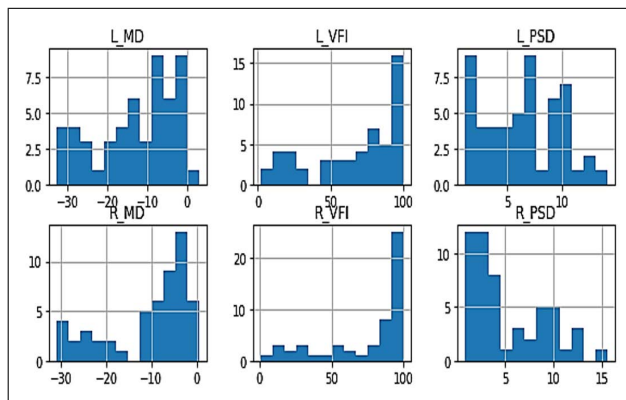


FIGURE 5. Histogram plot. L_MD and R_MD (left and right eye mean deviation), L_VFI and R_VFI (left and right eye visual field index), L_PSD and R_PSD (left and right eye pattern standard deviation).

based on the Visual Field Index (VFI) [26]. The higher severity grade is labeled in case each eye has different severity grades.

The distribution of data in different clinical measures are shown in the Figure 5. The descriptive statistics of clinical measures and p-value between glaucoma group and normal group are given in the Table 6.

EXGP features were validated with clinical features using Spearman Correlation Coefficient. Since visual search and

TABLE 6. Mean and standard deviation (in parenthesis) of age and clinical features and p-value between glaucoma group and normal group.

Clinical Information	Glaucoma (N=50)	Normal (N=48)	p-value
Age	54.9(13.7)	51.84(11.78)	0.264
L_MD	-12.0(9.5)	-3.04(2.34)	p<0.001
L_PSD	6.2(3.3)	1.94(0.94)	p<0.001
L_VFI	70.2(28.6)	97.26(3.14)	p<0.001
L_G	1.5(1.2)	3.51(1.70)	p<0.001
R_MD	-9.5(9.1)	-3.36(3.74)	p<0.001
R_PSD	4.8(3.7)	2.25(1.74)	p<0.001
R_VFI	78.2(28.2)	95.28(11.45)	p<0.001
R_G	2.0(1.5)	3.35(1.72)	p<0.001

free-viewing tasks were performed using both eyes, but clinical testing was performed for each eye, for validation purpose, clinical measures such as MD, PSD and VFI were taken for higher severity eye only.

Average Reaction Time is positively correlated with age 0.44. Convex hull area in visual search task is positively correlated with VFI of 0.42. Other EXGP features have weak correlation with clinical measures.

I. EXPLAINABLE DETECTION MODEL

Explainable Detection Model includes Deep Neural Network and Gaze Exploration Visualization. The explainability of the detection model is based on the contribution of different

TABLE 7. Summary of DNN architecture.

Layer	Shape	Activation	Parameters
Dense	28	ReLU	812
Dropout	28	-	0
Dense	24	ReLU	696
Dropout	24	-	0
Dense	22	ReLU	550
Dropout	22	-	0
Dense	2	-	46

features in generation of Gaze Exploration - index (GE-i) and the visualization of exploration tasks of different subgroups.

1) DEEP NEURAL NETWORK MODEL (DNN)

The eye gaze parameters and performance measures of visual exploration tasks unified to form EXGP feature set, which included 28 input parameters. The input feature vectors were fed to a sequential DNN model, which predicted the class label (glaucoma and normal).

Sequential DNN model is a stack of layers that produces output values based on the input feature vectors x_1, x_2, \dots, x_m , where m is the number of feature vectors. The input shape of the DNN model was 28 features in EXGP feature set. The feature set is fed in to 28, 24, 22 stack of fully connected (dense) layers with drop out value 0.5 at the end of every dense layers. Dropout technique helped to drop or retain the nodes for the next layer. Rectified Linear Unit (ReLU) activation function was applied to every dense layers to activate the nodes. ReLU is calculated as $f(x) = \max(0, x)$. The final dense layer outputs the probability between 0 and 1 with threshold 0.5. Class 0 referred as Normal and class 1 referred as Glaucoma.

The DNN model was compiled using Keras libraries with Tensorflow as the backend. Loss of the model was defined as mean squared error and optimizer as adam stochastic gradient descent algorithm. The model was fitted in the training dataset over 200 epochs. DNN model finally predicted on the test dataset and generated evaluation metrics such as accuracy score, sensitivity and specificity. The summary of the sequential model is given in the table 7.

The decision of the input shape or input features fed to the DNN model was based on SHapley Additive exPlanations (SHAP) KernelExplainer. KernelExplainer computed the relevance of each feature towards DNN model based on SHAP values. Postive SHAP values inferred that the feature has a positive impact towards the model, otherwise it has a negative impact towards the model. SHAP values were generated mathematically using (1).

$$\phi_i(f, x) = \sum_{z' \subseteq x'} \frac{(|z'| - 1)! (|x'| - |z'|)!}{(|x'|)!} (f_x(z') - f_x(z' \setminus i)) \quad (1)$$

Shapley value of feature vector fed to the model and is represented by $\phi_i(f, x)$. The Shapley value is calculated by taking all the permutations of different features in feature vector, x' . The permutation set of feature vector is represented by $|z'|$. The count of features in feature set is represented by

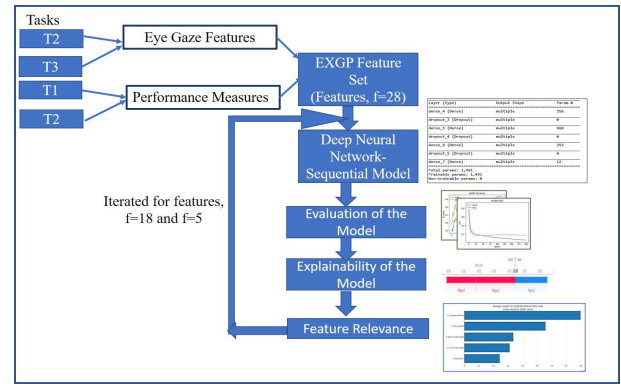


FIGURE 6. Workflow in explainable detection model.

$|x'|$ and $|z'|$. The relevance of each feature i in z' is considered by removing i^{th} feature in z' , which is represented by $f_x(z' \setminus i)$.

The Explainer() in the shap library returned the relevant features from the EXGP dataset. The relevant features fed to the DNN model and the performance of the model were evaluated for different iterations. Iteration in the detection model is the repeated selection of features from the EXGP dataset and estimation of performance metrics of DNN model after feeding the pertinent features in the model.

In iteration number, $t=1$, all 28 features i.e., $f=28$ in EXGP feature set were fed to DNN model. The model was evaluated based on criteria such as accuracy, sensitivity and specificity. The explainability of DNN model was checked based on KernelExplainer and top 10, i.e. $f=10$ which contributed towards evaluation were selected for iteration number, $t=2$. The evaluation metrics of the model were calculated and recorded. The final feature list which includes top 5 features, $f=5$ were selected and fed to DNN model in iteration number, $t= 3$. The final Explainable Detection Model for the prediction of glaucoma is based on top 5 features: fv_Convex Hull Area, star_Fix Conn Length, star_Avg FC, Dot_Avg Miss and fv_Fix Conn Length. The workflow pipeline in Explainable Detection Model is shown in the Figure 6.

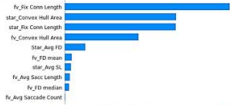

2) DASHBOARD

The explainability of the feature importance was amalgamated with an interactive dashboard using 'explainerdashboard' library. 'RegressionExplainer' performed explainability of final list of 5 features using scikit-learn based machine learning model on test data. The dashboard helped to answer different 'what if' questions by showing feature dependence plot, feature contribution plot and table based on actual class: glaucoma and normal. Certain weights were assigned to the relevant features to discriminate between glaucoma and normal. Thus a screening index called Gaze Exploration-index (GE-i) is generated.

3) VISUALIZATION

Another task of Explainable Detection Model was the visualization of gaze exploration. The pertinent or exploratory gaze

TABLE 8. Iterative improvement in accuracy of DNN model based on feature relevance.

Iteration, t	Count of Feature Relevance, f	Summary of Variable Importance Plot	Accuracy Score	Sensitivity	Specificity
t=1	f=28	-	0.61	1.0	0.093
t=2	f=10		0.74	0.944	0.23
t=3	f=5		0.80	1.0	0.75

patterns were visualized on to a single image. This helped to understand the difficult regions of participants during the performance of tasks.

Gaze Fusion Map (GFM) map was generated by fusing relevant information of 30 images [36]. It is the outcome of monocular performance of different participants by fusing ‘hit/miss’ of 30 images. The dark spot represents ‘not seen’ the target and red spot represents ‘seen’ the target.

Gaze Fusion Reaction Time (GFRT) map was generated by fusing relevant information or target on to a single image. Two variables such as hit/miss and reaction time during visual search task were overlaid onto the image. It is the outcome of binocular performance during 20 images. GFRT visualization helped to understand position of different targets, hit/miss of the target, and average reaction time.

Reaction time and miss of different participants visualized on to a single image, highlighted the difficult regions irrespective of exploratory gaze patterns.

IV. RESULTS

Gaze Exploration-index (GE-i) Explainable Detection Model is an interactive platform written in the collaborative notebook. The sample dataset included 98 cases, and 67% of the dataset was set as training dataset and 33% was set as a testing dataset. The Sequential Deep Neural Network (DNN) model fits the training dataset, and the accuracy score of the testing dataset is recorded after every iteration of feature relevance. The final list of 5 relevant features predicted the unseen samples and improved the accuracy score of the model to 0.80.

KernelExplainer on SHAP (SHapley Additive exPlanations) explained different attributes of the detection model. The summary plot of SHAP depicted the feature relevance in descending order. The accuracy of the DNN model is improved based on the relevant features given as input variables. In each iteration, f=28, f=10, and f=5 pertinent features of the training dataset were fed to the model and recorded the accuracy, sensitivity, and specificity. The summary plot of iterative improvement in the accuracy of the DNN model after feature relevance is shown in the table 8.

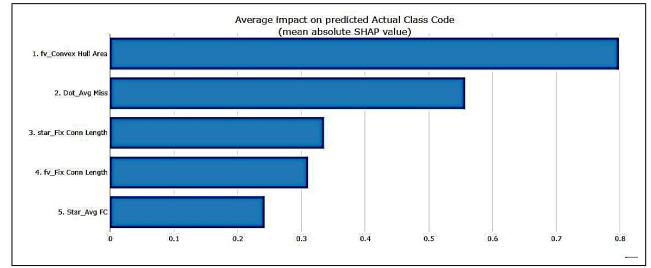


FIGURE 7. Feature relevance on detection model.

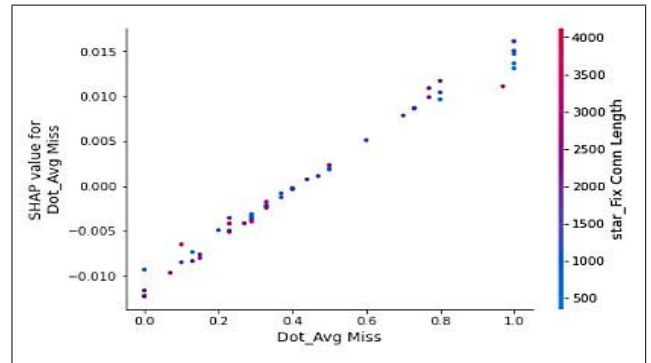


FIGURE 8. Feature interaction between dot_average miss and star_fixation connection length.

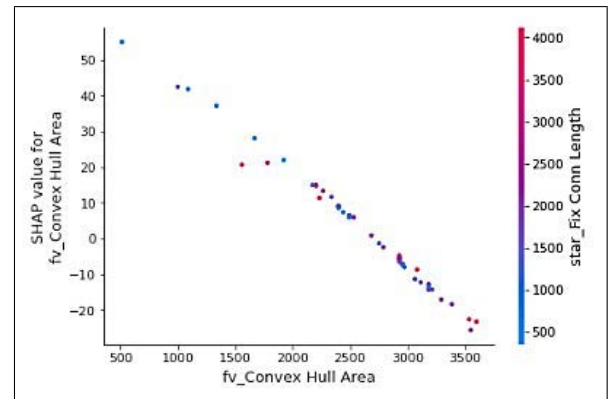


FIGURE 9. Feature interaction between fv_convex hull area and star_fixation connection length.

The final list of 5 relevant features are shown in the bar graph Figure 7.

A positive interaction existed between average miss during simple dot task and fixation connection length generated during visual search. The dependency plot between average miss and fixation length of visual search is shown in the Figure 8.

There is linear and negative trend between convex hull area and fixation connection length. The dependency plot between convex hull area generated during free-viewing task and fixation connection length during visual search is shown in the Figure 9.

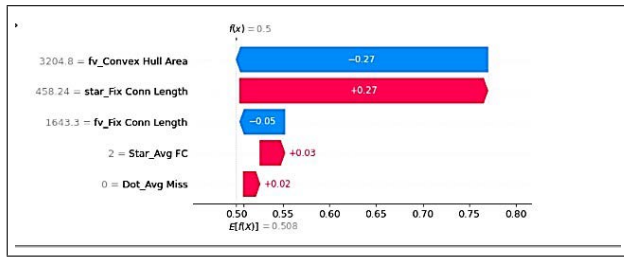


FIGURE 10. Water fall plot of feature relevance.

The waterfall plot shows the feature relevance towards the prediction of class. The waterfall plot of relevant features are depicted in the Figure 10. The base value or $E[f(X)]$ is the expected value that calculates the model output's average. Convex Hull Area estimated during the free-viewing task had a negative trend towards prediction result. Fixation connection length generated during the visual search task had a positive trend towards the prediction. Fixation count in visual search, fixation connection length generated during visual search task, and average miss in simple dot task had a positive trend towards the prediction result. Fixation connection length and convex hull area during the free-viewing task had a negative trend from the actual class label.

A. GAZE EXPLORATION VISUALIZATION

The comparison between fusion maps of study eye is shown in the figure 11. The fusion maps of three subgroups of glaucoma: severe, moderate and mild, and normal are shown in the figure. GFM map of severe glaucoma participant, Sub_73 showed more dark spots in the edges of the screen and towards the center. GFRT map of severe glaucoma participants did not identify the target in most of the stimuli, and reaction time was longer towards the edge of the screen. The subgroup showed restriction in the field of view with a limited number of fixations in the GFCH map. GFM map and GFRT map of moderate subgroup, Sub_42 showed that the miss of target is less than that of the severe subgroup. The reaction time to find out the target is longer towards the screen. GFCH map of moderate subgroup showed that the number of fixations are occupied on a specific part of the screen. The participant in the mild subgroup, Sub_97 showed less miss in simple-dot and visual search tasks than the severe and moderate subgroups. On the other hand, the GFCH map depicted that the moderate subgroup showed more fixations than higher severity subgroups. The normal group (Sub_86) could find almost all the target points in simple-dot and visual search tasks. The reaction time of the normal group during the visual search task is shorter than other subgroups of the glaucoma group. GFCH map of the normal group occupied more fixations overall portion of the screen without any restriction.

B. GAZE EXPLORATION - INDEX (GE- I)

A dashboard was created to reveal model explainability and to generate Gaze Exploration-index (GE-i). The final relevant

TABLE 9. Mean and standard deviation (in parenthesis) of GE-i value.

Measure	Normal	Glaucoma	p-value
GE-i value	-0.92(1.04)	0.50(0.82)	p<0.001

features are fv_Convex Hull Area, star_Fix Conn Length, star_Avg FC, Dot_Avg Miss and fv_Fix Conn Length. fv_Convex Hull Area showed high predictive power towards class label (Glaucoma and Normal). The equation is derived based on the weights formulated after regression equation. Gaze Exploration-Index (GE-i) is a single parameter based on the top 5 relevant features. GE-i equation is generated as in (2), significantly different between glaucoma and normal.

$$GE - i$$

$$= w_1 * fv_Convex\ Hull\ Area + w_2 * star_Fix\ Conn\ Length + w_3 * star_AvgFC + w_4 * Dot_Avg\ Miss + w_5 * fv_Fix\ Conn\ Length + b_0. \quad (2)$$

The mean and standard deviation of GE-i value of glaucoma and normal is shown in the Table 9. There is significant difference between glaucoma and normal in GE-i value. The box plot showed the distribution of GE-i of glaucoma and normal in the figure 12.

V. DISCUSSION

The Gaze Exploration-index (GE-i) Explainable Detection Model comprised data acquisition, estimation of performance and eye gaze parameters, explainable detection model, and generation of screening index. The visual exploration tasks were displayed on the screen to understand the exploratory eye movement patterns to compensate for the visual field loss. The feature extraction process included estimating basic eye gaze parameters using open source software and estimating derived parameters using customized software in the proposed model. The explainable detection model determined the relevant features for predicting glaucoma and generated a screening index on gaze exploration.

During visual exploration tasks, glaucoma participants showed a slower response in search tasks because of longer fixation duration. Simple dot task is a short trial time task, and hence the difference in the performance between glaucoma and normal is enormous. Nevertheless, glaucoma participants performed the task-oriented activity better than the free-viewing task. The decrease in the performance is due to longer fixation duration, and they did not respond within the trial time. However, the free-viewing task's restriction in eye movement behavior was explicitly seen due to less fixation count and shorter fixation connection length.

Analysis of EXGP parameters also enlightens compensatory eye gaze patterns among different glaucoma subgroups. Statistical measures showed that age reduced the effort of ignoring distractors and affected the performance of glaucoma participants during the simple-dot task and

Sub_Id	Class, Severity	Visual Field Map	GFM Map	GFRT Map	GCHM Map
Sub_73	G, Severe				
Sub_42	G, Moderate				
Sub_97	G, Mild				
Sub_86	G, Normal				

FIGURE 11. Comparison of fusion maps generated for different tasks.

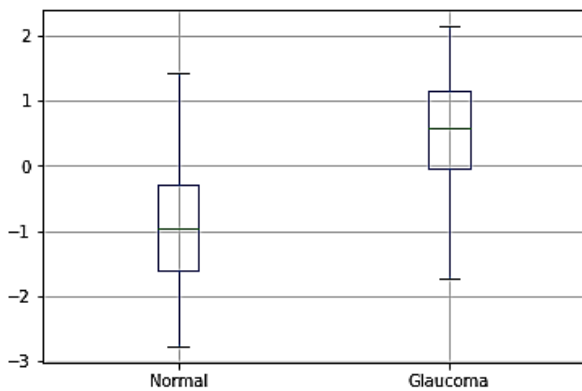


FIGURE 12. Box plot of GE-i value.

visual search task. Young glaucoma participants improved the search performance by coping with the difficulty by improving the frequency of fixation and its duration, neglecting their limitation in the field of view. Mild glaucoma or early-stage glaucoma patients showed many saccades to compensate for the visual field loss. The exploratory gaze patterns are involved in both free-viewing and visual search tasks. Elderly glaucoma participants show restricted eye movement behavior compared to middle-aged and young glaucoma participants.

Subgroup analysis of EXGP features highlights that visual exploration is worsened due to the impact of age rather than

severity. Restriction or convex hull area is positively correlated with the visual field index or the indicator of severity grade.

The pertinent features of each task was visualized onto fusion maps. Gaze Fusion Map (GFM) highlighted the monocular ability of search performance. The binocular performance of all glaucoma subgroups was improved due to compensatory eye movement patterns, which can be seen in the Gaze Fusion Reaction Time (GFRT) map. The visual processing was reduced during the free-viewing task which is depicted in Gaze Convex Hull Map (GCHM).

All EXGP features are initially fed to the deep learning model, and the performance is tuned based on the input of relevant features. The relevant features to discriminate between glaucoma and normal are present in different visual exploration tasks. In simple image-viewing tasks, glaucoma patients occupied their fixations in a limited field of view, and during task-oriented activity, they utilized compensatory eye movements in the form of more number of fixations and increased fixation connection length. All these features were dependent on each other and contributed to the detection of glaucoma.

A. TRUE CASE: NORMAL PREDICTION

Figure 13 (a) and 14 (a) showed the contribution table and plot of the top relevant EXGP features of a normal participant, Sub_44 respectively. The normal participant showed a large

Average of population	-0.76
Dot_Avg Miss = 0.29	-0.21
fv_Convex Hull Area = 2927.9	-0.21
star_Fix Conn Length = 2151.95	-0.12
fv_Fix Conn Length = 1188.79	-0.02
Star_Avg FC = 6.3	+0.01
Other features combined	+0.0
Final prediction	-1.3

(a) Sub_44 participant

Reason	Effect
Average of population	-0.76
fv_Convex Hull Area = 2137.79	+1.31
Dot_Avg Miss = 0.33	-0.13
star_Fix Conn Length = 2085.82	-0.1
fv_Fix Conn Length = 981.94	+0.08
Star_Avg FC = 6.22	+0.01
Other features combined	+0.0
Final prediction	0.41

(b) Sub_64 participant

Reason	Effect
Average of population	-0.76
fv_Convex Hull Area = 3678.44	-1.64
Dot_Avg Miss = 0.73	+0.71
star_Fix Conn Length = 1860.08	-0.02
fv_Fix Conn Length = 1976.71	-0.39
Star_Avg FC = 9.0	+0.2
Other features combined	+0.0
Final prediction	-1.91

(c) Sub_45 participant

Reason	Effect
Average of population	-0.76
fv_Convex Hull Area = 1366.46	+2.78
Dot_Avg Miss = 0.5	+0.23
star_Fix Conn Length = 653.94	+0.37
fv_Fix Conn Length = 162.99	+0.48
Star_Avg FC = 4.0	-0.15
Other features combined	+0.0
Final prediction	2.94

(d) Sub_75 participant

FIGURE 13. Contribution table of relevant features towards the prediction.

number of fixations in performing visual search tasks and free-viewing tasks and the average miss is less in the simple-dot task. FC in the free-viewing task showed a positive impact on the model.

B. FALSE PREDICTION AS GLAUCOMA

Figure 13 (b) and 14 (b) showed the contribution table and plot of the top relevant EXGP features of a normal participant, Sub_64 towards the final prediction. The participant is the middle-age normal group. The convex hull area parameter during the free-viewing task is less than the mean value of glaucoma. The fixation connection length during visual search and free-viewing tasks is shorter than that of glaucoma participants. Hence the GE-i Explainable Detection model has misclassified Sub_64 participant as a glaucoma participant.

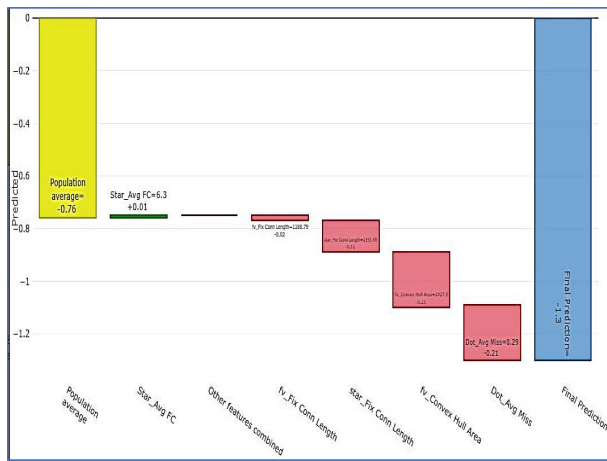
C. FALSE PREDICTION AS NORMAL

Figure 13 (c) and 14 (c) showed the contribution table and plot of the top relevant EXGP features of a glaucoma participant,

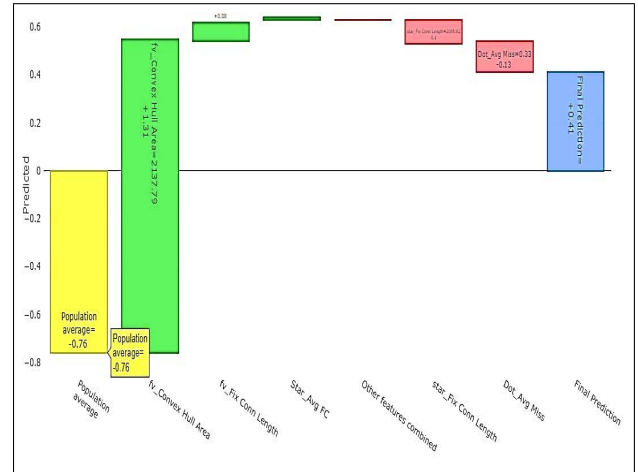
Sub_45 towards the final prediction. The severity of Sub_45 participant was severe in one eye and normal in another eye and belonged to the young age group. The explainable detection model misclassified the glaucoma participant as normal because the convex hull area is larger than the mean value of normal and fixation connection length in case both visual search and free-viewing task are longer, similar to normal. Since only one eye is affected with severe glaucoma and belonged to the young age group, the participant used compensatory eye movement patterns and showed more fixation count to find the target. Convex hull area also showed that they utilized a large portion of the screen to explore the images.

D. TRUE CASE: GLAUCOMA PREDICTION

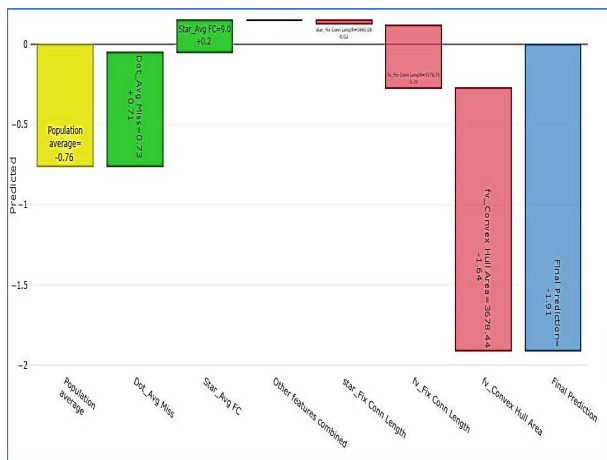
Figure 13 (d) and 14 (d) showed the contribution table and plot of the top relevant EXGP features of a glaucoma participant, Sub_75 towards the final prediction. The severity of Sub_75 participant was severe on both eyes and belonged to the middle age group. The value of relevant features shown by



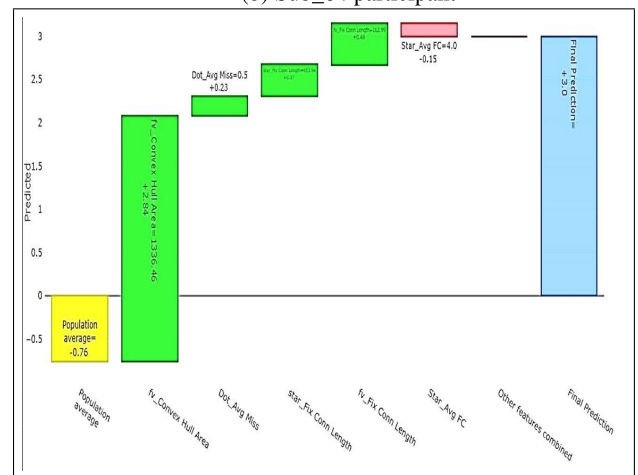
(a) Sub_44 participant



(b) Sub_64 participant



(c) Sub_45 participant



(d) Sub_75 participant

FIGURE 14. Contribution plot of relevant features towards the prediction.

Sub_75 are less than the mean value computed for glaucoma, and hence the features positively impact the model and are correctly predicted as glaucoma.

Young age group participants with no glaucoma condition in one of the eyes showed compensatory eye movements with more fixation counts in their defected visual field area.

In some previous works, Glaucoma Risk Index (GRI) was formulated [37]–[40], [41] based on clinical measures calculated on structural fundus images. The proposed work Gaze Exploration - index (GE-i) Explainable Detection Model is different from the previous works in the aspect of eye movement measures while viewing any visual exploration tasks. The proposed system focused on how the glaucoma group utilized the field of view in performing day-to-day tasks. GE-i is formulated based on the weights applied on the relevant features. The relevant features are taken based on the SHapley Additive exPlanations (SHAP) and the weights are generated using regression. The GE-i screening index discriminated glaucoma and normal based on the visual exploration on day-to-day tasks.

The system used a sequential deep learning model, and a dashboard is created to understand the model’s explainability and generate a screening index to understand visual exploration of glaucoma. However, since the exploratory gaze patterns were performed by young and early-stage glaucoma participants during visual search, there is a significant chance of a late diagnosis of disease. Therefore, the proposed system can probably be extended to modify the screening index to identify such subgroups and advise them for further diagnosis.

Thus the answers to the research questions are:

- 1) Are exploratory gaze patterns of the same participant reflect in all tasks? No, the same participant did not show the same exploratory gaze pattern in all tasks. Visual exploration is performed more during goal-oriented activity than the free-viewing task. Young glaucoma and early-stage glaucoma participants showed more fixations and longer fixation duration in goal-oriented activity or visual search, ignoring the visual field defect. Age is also a

critical factor in the involvement of exploratory gaze patterns.

- 2) What are the relevant eye gaze measures and performance measures that contribute the prediction of glaucoma?

The relevant features to design the detection model are convex hull area and fixation count. This depicts restriction in the field of view. Fixation connection length in any task reveals gaze orientation of finding the target or salient features. Performance measure of simple dot task correctly discriminates between the defected and less defected eye.

- 3) Can we formulate screening index that discriminates glaucoma and normal?

Yes, finally the detection model generated screening index based on the weights applied to different 5 features. Convex hull area has given more weight than other relevant features. The exploration index significantly discriminates between glaucoma and normal.

VI. CONCLUSION

The proposed system Gaze Exploration - index (GE-i) is Computer-Aided Detection (CADE) model for glaucoma. It is a blend of screening index for visual exploration and visualization of the influence of severity and age in eye movement behavior. The explainability and estimation of exploratory gaze patterns depict that exploratory gaze patterns have pertained in visual search than simple image viewing. The devised screening index discriminates glaucoma and normal and helps to utilize the knowledge of compensatory eye gaze patterns to cease the decline in their quality of life.

REFERENCES

- [1] S. Dubey, H. Bedi, M. Bedi, P. Matah, J. Sahu, S. Mukherjee, and L. Chauhan, "Impact of visual impairment on the wellbeing and functional disability of patients with glaucoma in India," *J. Current Ophthalmol.*, vol. 32, no. 1, p. 14, Nov. 2019.
- [2] E. W. Chan, X. Li, Y.-C. Tham, J. Liao, T. Y. Wong, T. Aung, and C.-Y. Cheng, "Glaucoma in Asia: Regional prevalence variations and future projections," *Brit. J. Ophthalmol.*, vol. 100, no. 1, pp. 78–85, Jan. 2016.
- [3] S. J. Leat and J. E. Lovie-Kitchin, "Visual function, visual attention, and mobility performance in low vision," *Optometry Vis. Sci.*, vol. 85, no. 11, pp. 1049–1056, 2008.
- [4] C. M. Chisholm, F. G. Rauscher, D. C. Crabb, L. N. Davies, M. C. Dunne, D. F. Edgar, J. A. Harlow, M. James-Galton, A. Petzold, G. T. Plant, A. C. Viswanathan, G. J. Underwood, and J. L. Barbur, "Assessing visual fields for driving in patients with paracentral scotomata," *Brit. J. Ophthalmol.*, vol. 92, no. 2, pp. 225–230, Feb. 2008.
- [5] E. David, J. Beitner, and M. L.-H. Vö, "Effects of transient loss of vision on head and eye movements during visual search in a virtual environment," *Brain Sci.*, vol. 10, no. 11, p. 841, Nov. 2020.
- [6] P. A. Grasso, E. Lädavas, and C. Bertini, "Compensatory recovery after multisensory stimulation in hemianopic patients: Behavioral and neurophysiological components," *Frontiers Syst. Neurosci.*, vol. 10, p. 45, May 2016.
- [7] E. Kasneci, K. Sippel, K. Aehling, M. Heister, W. Rosenstiel, U. Schiefer, and E. Papageorgiou, "Driving with binocular visual field loss? A study on a supervised on-road parcours with simultaneous eye and head tracking," *PLoS ONE*, vol. 9, no. 2, Feb. 2014, Art. no. e87470.
- [8] K. Ball, C. Owsley, M. E. Sloane, D. L. Roenker, and J. R. Bruni, "Visual attention problems as a predictor of vehicle crashes in older drivers," *Investigative Ophthalmol. Vis. Sci.*, vol. 34, no. 11, pp. 3110–3123, 1993.
- [9] P. K. Nirmalan, J. M. Tielsch, J. Katz, R. D. Thulasiraj, R. Krishnadas, R. Ramakrishnan, and A. L. Robin, "Relationship between vision impairment and eye disease to vision-specific quality of life and function in rural India: The Aravind comprehensive eye survey," *Investigative Ophthalmol. Vis. Sci.*, vol. 46, no. 7, pp. 2308–2312, 2005.
- [10] H. Kumar, S. Monira, and A. Rao, "Causes of missed referrals to low-vision rehabilitation services: Causes in a tertiary eye care setting," *Seminars Ophthalmol.*, vol. 31, no. 5, pp. 452–458, 2016.
- [11] V. K. Gothwal, D. K. Bagga, H. L. Rao, S. Bharani, R. Sumalini, C. S. Garudadri, S. Senthil, S. P. Reddy, V. Pathak-Ray, and A. K. Mandal, "Is utility-based quality of life in adults affected by glaucoma?" *Investigative Ophthalmol. Vis. Sci.*, vol. 55, no. 3, pp. 1361–1369, 2014.
- [12] Y. S. Kim, M. Y. Yi, Y. J. Hong, and K. H. Park, "The impact of visual symptoms on the quality of life of patients with early to moderate glaucoma," *Int. Ophthalmol.*, vol. 38, no. 4, pp. 1531–1539, Aug. 2018.
- [13] A. Azuara-Blanco and J. Burr, "The rising cost of glaucoma drugs," *Brit. J. Ophthalmol.*, vol. 90, no. 2, pp. 130–131, Feb. 2006.
- [14] C. Owsley and G. McGwin, "Vision impairment and driving," *Surv. Ophthalmol.*, vol. 43, no. 6, pp. 535–550, May 1999.
- [15] E. Wiecek, L. R. Pasquale, J. Fiser, S. Dakin, and P. J. Bex, "Effects of peripheral visual field loss on eye movements during visual search," *Frontiers Psychol.*, vol. 3, p. 472, Nov. 2012.
- [16] S. S.-Y. Lee, A. A. Black, and J. M. Wood, "Effect of glaucoma on eye movement patterns and laboratory-based hazard detection ability," *PLoS ONE*, vol. 12, no. 6, Jun. 2017, Art. no. e0178876.
- [17] D. P. Crabb, N. D. Smith, and H. Zhu, "What's on TV? Detecting age-related neurodegenerative eye disease using eye movement scanpaths," *Frontiers Aging Neurosci.*, vol. 6, p. 312, Nov. 2014.
- [18] D. S. Asfaw, P. R. Jones, V. M. Mönter, N. D. Smith, and D. P. Crabb, "Does glaucoma alter eye movements when viewing images of natural scenes? A between-eye study," *Investigative Ophthalmol. Vis. Sci.*, vol. 59, no. 8, pp. 3189–3198, 2018.
- [19] E. Kasneci, K. Sippel, K. Aehling, M. Heister, W. Rosenstiel, U. Schiefer, and E. Papageorgiou, "Driving with binocular visual field loss? A study on a supervised on-road parcours with simultaneous eye and head tracking," *PLoS ONE*, vol. 9, no. 2, Feb. 2014, Art. no. e87470.
- [20] T. C. Kübler, E. Kasneci, W. Rosenstiel, M. Heister, K. Aehling, K. Nagel, U. Schiefer, and E. Papageorgiou, "Driving with glaucoma: Task performance and gaze movements," *Optometry Vis. Sci.*, vol. 92, no. 11, pp. 1037–1046, 2015.
- [21] F. Vargas-Martín and E. Peli, "Eye movements of patients with tunnel vision while walking," *Investigative Ophthalmol. Vis. Sci.*, vol. 47, no. 12, pp. 5295–5302, 2006.
- [22] S. S.-Y. Lee, A. A. Black, and J. M. Wood, "Effect of glaucoma on eye movement patterns and laboratory-based hazard detection ability," *PLoS ONE*, vol. 12, no. 6, Jun. 2017, Art. no. e0178876.
- [23] R. P. Vega, P. M. van Leeuwen, E. R. Vélaz, H. G. Lemij, and J. C. F. de Winter, "Obstacle avoidance, visual detection performance, and eye-scanning behavior of glaucoma patients in a driving simulator: A preliminary study," *PLoS ONE*, vol. 8, no. 10, Oct. 2013, Art. no. e77294.
- [24] T. C. Kübler, E. Kasneci, W. Rosenstiel, M. Heister, K. Aehling, K. Nagel, U. Schiefer, and E. Papageorgiou, "Driving with glaucoma: Task performance and gaze movements," *Optometry Vis. Sci.*, vol. 92, no. 11, pp. 1037–1046, 2015.
- [25] T. C. Kübler, E. Kasneci, W. Rosenstiel, U. Schiefer, K. Nagel, and E. Papageorgiou, "Stress-indicators and exploratory gaze for the analysis of hazard perception in patients with visual field loss," *Transp. Res. F, Traffic Psychol. Behav.*, vol. 24, pp. 231–243, May 2014.
- [26] K. Sippel, E. Kasneci, K. Aehling, M. Heister, W. Rosenstiel, U. Schiefer, and E. Papageorgiou, "Binocular glaucomatous visual field loss and its impact on visual exploration—A supermarket study," *PLoS ONE*, vol. 9, no. 8, Aug. 2014, Art. no. e106089.
- [27] N. D. Smith, D. P. Crabb, F. C. Glen, R. Burton, and D. F. Garway-Heath, "Eye movements in patients with glaucoma when viewing images of everyday scenes," *Seeing Perceiving*, vol. 25, no. 5, pp. 471–492, Jul. 2012.
- [28] I. V. Ivanov, M. Mackeben, A. Vollmer, P. Martus, N. X. Nguyen, and S. Trauzettel-Klosinski, "Eye movement training and suggested gaze strategies in tunnel vision—A randomized and controlled pilot study," *PLoS ONE*, vol. 11, no. 6, Jun. 2016, Art. no. e0157825.
- [29] G. Luo, F. Vargas-Martín, and E. Peli, "The role of peripheral vision in saccade planning: Learning from people with tunnel vision," *J. Vis.*, vol. 8, no. 14, p. 25, 2008.

- [30] G. Luo, F. Vargas-Martin, and E. Peli, "The role of peripheral vision in saccade planning: Learning from people with tunnel vision," *J. Vis.*, vol. 8, no. 14, pp. 1–18, 2008.
- [31] W. Grundler and H. Strasburger, "Visual attention outperforms visual-perceptual parameters required by law as an indicator of on-road driving performance," *PLoS ONE*, vol. 15, no. 8, Aug. 2020, Art. no. e0236147.
- [32] R. Hemelings, B. Elen, J. Barbosa-Breda, M. B. Blaschko, P. De Boever, and I. Stalmans, "Deep learning on fundus images detects glaucoma beyond the optic disc," *Sci. Rep.*, vol. 11, no. 1, pp. 1–12, Dec. 2021.
- [33] S. Oh, Y. Park, K. J. Cho, and S. J. Kim, "Explainable machine learning model for glaucoma diagnosis and its interpretation," *Diagnostics*, vol. 11, no. 3, p. 510, Mar. 2021.
- [34] Y. Hagiwara, J. E. W. Koh, J. H. Tan, S. V. Bhandary, A. Laude, E. J. Ciaccio, L. Tong, and U. R. Acharya, "Computer-aided diagnosis of glaucoma using fundus images: A review," *Comput. Methods Programs Biomed.*, vol. 165, pp. 1–12, Oct. 2018.
- [35] S. Krishnan, J. Amudha, and S. Tejwani, "Intelligent-based decision support system for diagnosing glaucoma in primary eyecare centers using eye tracker," *J. Intell. Fuzzy Syst.*, vol. 41, no. 5, pp. 5235–5242, Nov. 2021.
- [36] S. Krishnan, J. Amudha, and S. Tejwani, "Gaze fusion-deep neural network model for glaucoma detection," in *Proc. Symp. Mach. Learn. Meta-heuristics Algorithms, Appl.* Singapore: Springer, 2020, pp. 42–53.
- [37] Y. Hagiwara, J. E. W. Koh, J. H. Tan, S. V. Bhandary, A. Laude, E. J. Ciaccio, L. Tong, and U. R. Acharya, "Computer-aided diagnosis of glaucoma using fundus images: A review," *Comput. Methods Programs Biomed.*, vol. 165, pp. 1–12, Oct. 2018.
- [38] M. R. K. Mookiah, U. R. Acharya, C. K. Chua, C. M. Lim, E. Y. K. Ng, and A. Laude, "Computer-aided diagnosis of diabetic retinopathy: A review," *Comput. Biol. Med.*, vol. 43, no. 12, pp. 2136–2155, 2013.
- [39] U. R. Acharya, S. Dua, X. Du, V. S. Sree, and C. K. Chua, "Automated diagnosis of glaucoma using texture and higher order spectra features," *IEEE Trans. Inf. Technol. Biomed.*, vol. 15, no. 3, pp. 449–455, May 2011.
- [40] J. Nayak, R. Acharya, P. S. Bhat, N. Shetty, and T.-C. Lim, "Automated diagnosis of glaucoma using digital fundus images," *J. Med. Syst.*, vol. 33, no. 5, pp. 337–346, Oct. 2009.
- [41] U. Raghavendra, H. Fujita, S. V. Bhandary, A. Gudigar, J. H. Tan, and U. R. Acharya, "Deep convolution neural network for accurate diagnosis of glaucoma using digital fundus images," *Inf. Sci.*, vol. 441, pp. 41–49, May 2018.
- [42] M. Sushil, G. Suguna, R. Lavanya, and M. N. Devi, "Performance comparison of pre-trained deep neural networks for automated glaucoma detection," in *Proc. Int. Conf. ISMAC Comput. Vis. Bio-Eng.* Cham, Switzerland: Springer, 2018, pp. 631–637.
- [43] G. Suguna and R. Lavanya, "Performance assessment of EyeNet model in glaucoma diagnosis," *Pattern Recognit. Image Anal.*, vol. 31, no. 2, pp. 334–344, Apr. 2021.
- [44] V. Srinithi and R. Lavanya, "Novel colour derivative based approach for CDR estimation in glaucoma diagnosis," in *Proc. 3rd Int. Conf. Trends Electron. Informat. (ICOEI)*, Apr. 2019, pp. 69–73.
- [45] S. S. Poorna, S. Anjana, P. Varma, A. Sajjeev, K. C. Arya, S. Renjith, and G. J. Nair, "Facial emotion recognition using DWT based similarity and difference features," in *Proc. 2nd Int. Conf. I-SMAC (IoT Social, Mobile, Analytics Cloud) (I-SMAC)/I-SMAC (IoT Social, Mobile, Analytics Cloud) (I-SMAC)*, 2nd Int. Conf., Aug. 2018, pp. 524–527.
- [46] R. Krishnan, V. Sekhar, J. Sidharth, S. Gautham, and G. Gopakumar, "Glaucoma detection from retinal fundus images," in *Proc. Int. Conf. Commun. Signal Process. (ICOSP)*, Jul. 2020, pp. 628–631.
- [47] O. Deperlioglu, U. Kose, D. Gupta, A. Khanna, F. Giampaolo, and G. Fortino, "Explainable framework for glaucoma diagnosis by image processing and convolutional neural network synergy: Analysis with doctor evaluation," *Future Gener. Comput. Syst.*, vol. 129, pp. 152–169, Apr. 2022.
- [48] K. Shankar, A. R. W. Sait, D. Gupta, S. K. Lakshmanaprabu, A. Khanna, and H. M. Pandey, "Automated detection and classification of fundus diabetic retinopathy images using synergic deep learning model," *Pattern Recognit. Lett.*, vol. 133, pp. 210–216, May 2020.
- [49] M. C. C. Sousa, L. G. Biteli, S. Dorairaj, J. S. Maslin, M. T. Leite, and T. S. Prata, "Suitability of the visual field index according to glaucoma severity," *J. Current Glaucoma Pract.*, vol. 9, no. 3, p. 65, 2015.
- [50] A. Voßkühler, V. Nordmeier, L. Kuchinke, and A. M. Jacobs, "OGAMA (open gaze and mouse analyzer): Open-source software designed to analyze eye and mouse movements in slideshow study designs," *Behav. Res. Methods*, vol. 40, no. 4, pp. 1150–1162, Nov. 2008.
- [51] A. Borji and L. Itti, "CAT2000: A large scale fixation dataset for boosting saliency research," 2015, *arXiv:1505.03581*.



SAJITHA KRISHNAN received the B.Tech. degree in computer science and engineering from the University of Calicut, in 2009, and the M.Tech. degree in computer vision and image processing from Amrita Vishwa Vidyapeetham University, Bengaluru, India, in 2012, where she is currently pursuing the Ph.D. degree in computer science and engineering. Her research interests include human–computer interaction, eye gaze analytics, and image and vision computing.



J. AMUDHA received the B.E. degree in electrical and electronics engineering from the Amrita Institute of Technology and Science, Coimbatore, India, in 1998, the M.E. degree in computer science and engineering, Anna University, Chennai, India, in 2002, and the Ph.D. degree in computer science and engineering from Amrita University, Coimbatore, in 2012.

She is currently a Professor with the Department of Computer Science, Amrita School of Engineering, Bengaluru. She is the member of UG and PG Board of Studies Member, NAAC Accreditation, and a NBA Committee Member. She has filed patent on an innovative technology in eye tracking research to automate the detection of optic disc for health care diagnostic systems. Her research interests include image processing, computer vision, soft computing, computational visual attention systems, cognitive vision, pattern recognition, and attention allocation in various fields, such as marketing and robotics.



SUSHMA TEJWANI received the degree in medical training from the Postgraduate Institute of Medical Sciences, Rohtak, in 1999. She was a Faculty Member at LVPEI, from 2003 to 2007, where she was actively involved in the education and training programs and headed the LVP-Zeiss Academy. She has undergone short term training for glaucoma with Dr. Arthur Sit at Mayo clinic, Rochester, USA, in 2007.

She has been working as the Consultant and the Head of Glaucoma Services with Narayana Nethralaya-2, Narayana Health City, Bangalore, since July 2007. She is actively involved in implementing NABH quality standards and has been working as an Accreditation Co-Coordinator with Narayana Nethralaya-2, since 2010. She is also an external part time Ph.D. Research Scholar with VIT University, Vellore. She has presented as a Faculty Member at more than 100 national and international meetings. She is a principal investigator with the part of many prestigious clinical trials. She has 37 publications in peer-reviewed journals and has also written few book chapters. Her research interests include glaucoma shunts, biomechanics in glaucoma, pediatric glaucoma, and refractive cataract surgeries.

Dr. Tejwani received the fellowship in comprehensive ophthalmology at the L.V. Prasad Eye Institute, from 2000 to 2003. She is a Reviewer of *Indian Journal of Ophthalmology (IJO)*, *Journal of Glaucoma* and *Journal of Ophthalmology*. She has received multiple awards, including the IJO Silver Award and the DB Chandra Disha Award.

• • •